The Report Committee for Farris Ahmad Bar
Certifies that this is the approved version of the following report:

Design and Production of an Energy Harvesting Wireless Sensor

APPROVED BY
SUPERVISING COMMITTEE:

Supervisor:

Jacob Abraham

Shouli Yan

Design and Production of an Energy Harvesting Wireless Sensor

by

Farris Ahmad Bar, BSEE

Report

Presented to the Faculty of the Graduate School of
The University of Texas at Austin
in Partial Fulfillment
of the Requirements
for the Degree of

Master of Science in Engineering

The University of Texas at Austin
May 2013

Dedication

To my daughter, Mariam, who has inspired me in so many ways.

Acknowledgements

I would like to express my deep appreciation to my project supervisor, Jacob Abraham and to the supervising committee member, Shouli Yan for their constructive feedback and support throughout the project. I would also like to thank Silicon Laboratories, in particular, Brent Wilson, for mentoring me early in my career and for approving work on this project when it was only an idea and for providing the support and resources to turn the idea into a marketable product.

I am grateful for my family, friends, co-workers, professors, supervisors, and anyone who has supported me either financially, with time and advice, or by providing moral support in completing my master's degree. I am also thankful to God for making this road possible for me and for providing me the health and wisdom to persevere in life and achieve my goals.

Abstract

Design and Production of an Energy Harvesting Wireless Sensor

Farris Ahmad Bar, M.S.E.
The University of Texas at Austin, 2013

Supervisor: Jacob Abraham

The widespread deployment of wireless sensors in our homes, offices, factories and infrastructure has opened the door for system designers to create novel approaches for powering wireless sensor nodes. In recent years, energy harvesting has emerged as the power supply of choice for embedded system designers, enabling wireless sensors to be used in applications that previously were not feasible with conventional battery-powered designs. This report details the design and development of an energy harvesting wireless sensor from concept to production. Design constraints included the requirement to operate reliably in a wide variety of environments, the use of commercially available components, and a visually appealing form factor. The result is a very power-efficient, solar-powered wireless sensor that measures temperature, voltage, and illumination level at the solar cell and has an ultra slim form factor.

Table of Contents

List of Figures

BACKGROUND

Chapter 1: Introduction

The widespread deployment of wireless sensors in our homes, offices, factories and infrastructure has opened the door for system designers to create novel approaches for powering wireless sensor nodes. In recent years, energy harvesting has emerged as the power supply of choice for embedded system designers, enabling wireless sensors to be used in applications that previously were not feasible with conventional battery-powered designs. The main objective of this project is to design and produce a self-sustaining wireless sensor that could operate perpetually using energy harvested from the environment. Design constraints include the requirement to operate reliably in a wide variety of environments, the use of commercially available components, and a visually appealing form factor.

Chapter 2: Prior Work

STATE OF THE ART IN ENERGY HARVESTING

Energy harvesting has been is a widely researched topic for many years and many researchers have created systems that can achieve perpetual operation. Most fully functioning embedded system designs that utilize energy harvesting power sources have been built in small quantities as proof of concept. This work mates the state of the art in commercially available energy harvesters and the latest advances in ultra-low-power embedded system design to achieve a mass-produced energy harvesting system.

SUMMER PROJECT -- ENERGY HARVESTING FOR HIGH DRAIN APPLICATIONS

This work builds on the survey and feasibility study of energy harvesting for high drain applications completed in August 2010. That work concluded that solar energy harvesting had the highest potential of being implemented in mass-produced electronics primarily due to its high power density when compared with other energy harvesting mediums. It also identified thin-film batteries as one of the types of energy storage devices that are most suitable for energy harvesting systems due to their low leakage characteristics. The summer project report may be obtained by contacting the author.

RF TO USB REFERENCE DESIGN

The Silicon Laboratories RF-to-USB reference design represents the state of the art in commercially available ultra-low-power wireless microcontrollers. It is built around an Si1014 wireless microcontroller capable of being powered from a supply voltage as low as 0.9 volts and only requires 60 nA of supply current to preserve state in its low power sleep mode. The Si1014 includes an RF transceiver that can operate in the 915 MHz ISM band and has industry leading transmit power and receive sensitivity specifications allowing it to communicate over an exceptionally long range.

The RF-to-USB reference design hardware, shown in Figure 2.A, includes a USB dongle that can receive data from multiple wireless nodes. The USB dongle plugs into a PC and transfers data received over RF to a graphic user interface (GUI) running on the PC. The GUI, shown in Figure 2.B, displays the current temperature at each node and the potentiometer value reported by the wireless devices.

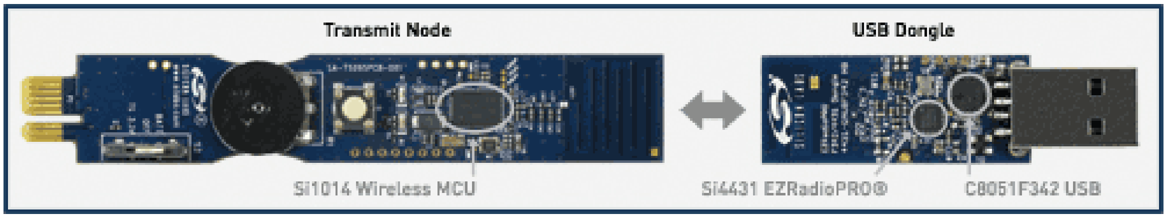

Figure 2.A: Silicon Laboratories RF-to-USB Reference Design Hardware

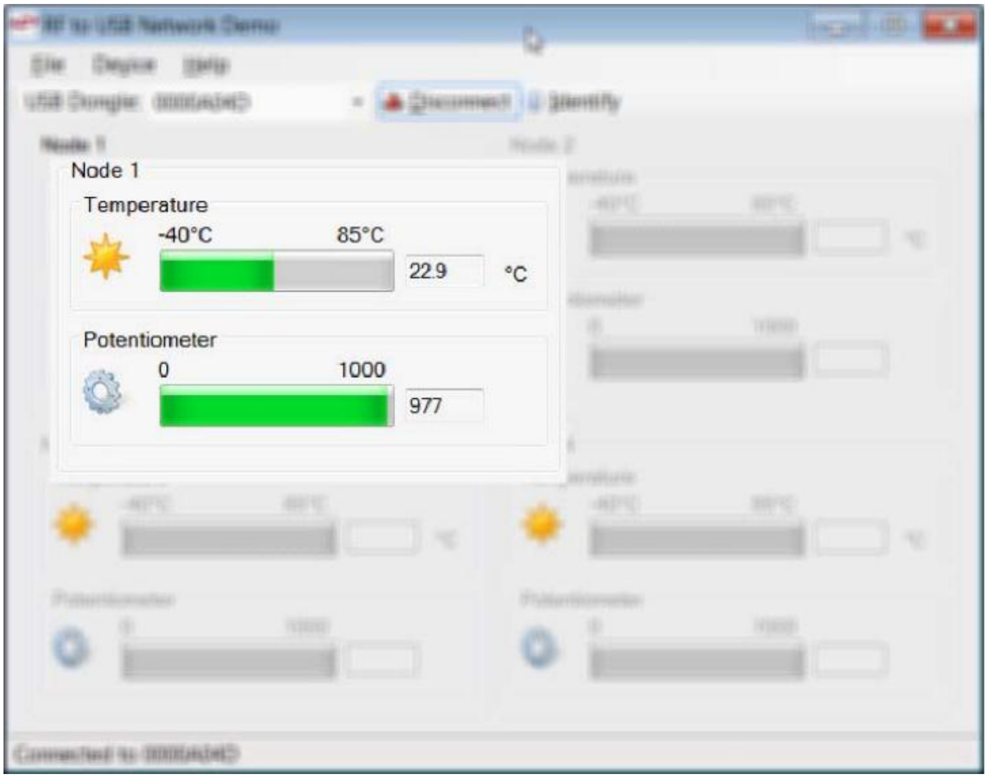

Figure 2.B: Silicon Laboratories RF-to-USB Reference Design PC Software

PROTOTYPE AND PROOF OF CONCEPT

The Silicon Labs RF-to-USB reference design was used as the starting point for prototyping the energy harvesting system. The RF-to-USB node was glued to a PCB with a large prototyping area, shown in Figure 2.C, for mechanical stability and additional circuitry was added to provide a debug connection to the MCU for firmware development, current measurement capability for characterizing system power, and alternate power options.

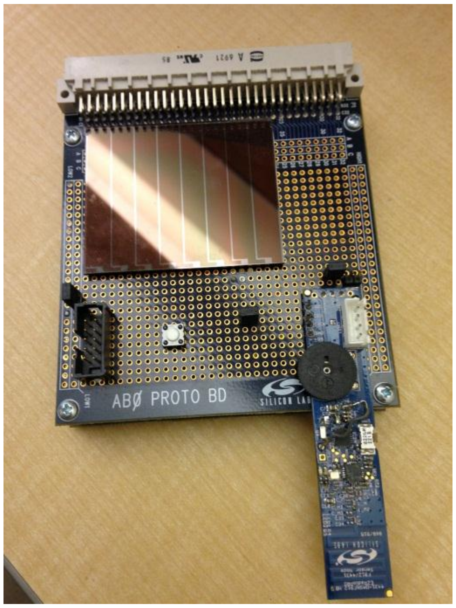

Figure 2.C: Energy Harvesting Prototype System

Although the prototype system was not optimized for energy harvesting and could not run perpetually, it was an excellent proof of concept vehicle that allowed rapid firmware development, experimentation with various power sources and energy storage devices, and provided confidence that perpetual operation could be achieved in a commercially available solution with additional optimization and energy balancing.

Chapter 3: Design Goals

At the outset of any embedded system design, a clear set of goals and requirements are established to ensure the end product meets the needs for which it was created. The design goals of this energy harvesting embedded system are discussed in the following paragraphs.

RELIABILITY AND ROBUSTNESS

To achieve commercial success, an embedded system must be reliable and robust. Embedded systems are used in everything from home thermostats to medical devices and the general population has come to depend on embedded systems for performing everyday tasks. Further, energy harvesting systems are often used to replace traditional battery powered systems that are difficult or very costly to service.

The requirement for reliability and robustness affects decisions taken early in the design process, such as component selection, building in the necessary design margin to ensure proper operation in varying environmental conditions, and taking a conservative approach in designing and testing the firmware. Reliability and robustness are excellent goals for any embedded system design.

FORM FACTOR

With each new generation of embedded system designs, form factors continue to shrink. The general population has come to expect that each new iteration of a product will be smaller and more powerful than the one before it. System designers looking to replace traditional battery powered designs with energy harvesting systems need a solution with a slim form factor that is visually appealing to the end customer.

EASE OF USE

To ensure that an embedded system is useful in the hands of the end customer and does not overwhelm the support team with service calls, it is important that it have an easy to use interface. One of the design goals of this project is to have a simple and user friendly interface.

RANGE

In RF systems, range increases with transmit power and system designers try to maximize transmit power in order to achieve maximum range. For a power constrained system, the system designer chooses the minimum transmit power that will achieve the required range. This design has a minimum required range of 10 meters.

INTEROPERABILITY AND MULTI-NODE CAPABILITY

The RF nodes in this design must be able to interoperate with one another and the receiver must be able to receive data from multiple nodes. This will require each node to have a unique address so that the receiver would be able to identify which transmitter sent the packet. The receiver must be able to support reception from up to 4 nodes.

MANUFACTURABILITY AND COMPONENT AVAILABILITY

This system is intended to be mass-produced and must therefore use only commercially available components. Long lead time components should be used sparingly to minimize the impact of lead time on inventory management.

SYSTEM DESIGN

Chapter 4: Power Supply

The power supply is the heart of an energy harvesting system and it is what keeps it in continuous operation. A well designed power supply will meet the power needs of the system with minimum conversion loss. This energy harvesting system has a sophisticated power supply that utilizes solar energy to meet its power needs and enable it to achieve perpetual operation.

HARVESTING SOURCE

The project requirements specify a solar energy harvesting supply that is built from commercially available components. A number of solar cell vendors were examined and Sanyo was selected to be the vendor to provide the solar cells for this design because of availability, performance, and cost.

Several solar cells from the Amorton line were evaluated and the AM-1815 was selected because it could provide 126 μW at 200 lx and much higher power levels at increasing illumination levels. The size of the cell was very reasonable measuring 58.1 x 48.6 mm and it is widely available on the market at a cost of approximately 4 USD per cell in 1000 piece quantities.

ENERGY STORAGE

Based on previous work, the two energy storage technologies most suitable for energy harvesting applications are lithium ion batteries and thin film batteries. Since form factor is important in this design, the MEC-101 700 μA-H thin film battery from Infinite Power Solutions was selected to perform energy storage in this design.

OUTPUT POWER REQUIREMENTS

The output power requirements of this supply can be classified into a static and a dynamic component. The static component is based on the average supply current of the load. If the power supply is designed such that it can source 100 µA of average current continuously over a period of at least one hour, it would fully meet the static power requirements of the system.

The dynamic power requirements are quite higher since the system will need to power an RF transmitter for short periods of time. The peak current should be designed to be in the range of 30 to 50 mA for at least two milliseconds. A large decoupling capacitor has been placed on the power supply output to source the dynamic energy requirements of system. The required capacitor size is determined by the duration of the required current pulse and this topic is discussed further in Chapter 7.

POWER ON RESET

Most embedded systems require significantly more energy to get through a power-on reset than during normal operation. Although this is typically a one-time event and does not factor into the system's steady state energy requirements, it is necessary to design the system with the ability to recover in case of a power failure, power down event, or it is placed in storage for a prolonged period of time.

The problem with a power on reset in energy harvesting systems is that the energy harvesting power supply typically will not be able to supply enough instantaneous energy to get the system through a power-on reset. This will place the system in an infinite loop trying to start up without ever being able to fully energize the system. To survive the initial power-on reset, an energy harvesting system must delay the start of the power-on reset until it is able to accumulate sufficient energy in a capacitor to get the system through the reset.

Figure 4.A shows a circuit architecture that can enable a power-hungry embedded system to go through a power-on reset using only harvested energy. Starting from the unpowered state, the primary energy storage element is disconnected from the system by a battery protection circuit. The energy harvester alone charges the capacitor, which will later be used to supply energy for the power-on reset. A supply voltage monitor and regulator gate the power supply to the embedded system to minimize its power consumption while the capacitor is charging.

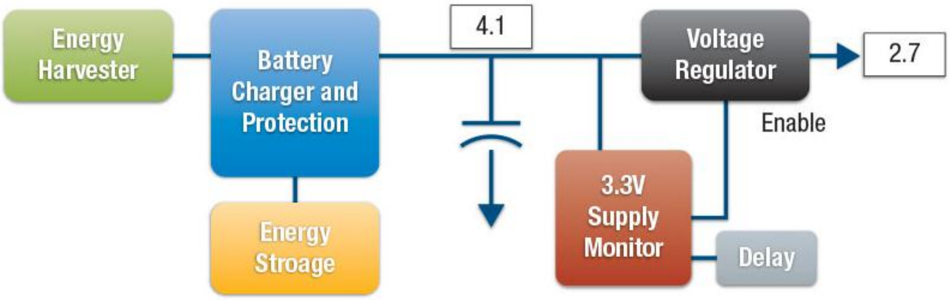

Figure 4.A: Gathering sufficient energy to overcome the power-on reset

After some time, the capacitor voltage will reach a trip point that triggers the supply monitor to initiate the power-on reset sequence. The supply monitor ideally has a programmable delay that provides additional time for the capacitor to charge prior to enabling power to the embedded system. When the voltage regulator is enabled, the capacitor is discharged into the embedded system, allowing it to complete its power-on reset and enter a low-power sleep mode. Once the battery charger detects sufficient voltage on the input capacitor, it reconnects the energy storage element to the system, and the energy harvesting system is in full operation. This circuit was implemented in this design and a full schematic can be found in the appendix.

BATTERY CHARGER AND PROTECTION

The battery charger used in this design is a shunt charger that guarantees that the charge voltage does not exceed 4.1 V. It also disconnects the battery if its voltage drops below 2.7V to protect it from over discharge.

LEAKAGE

The shunt charger and LDO in this design must remain enabled in order to harvest energy. The leakage as a result of enabling the charger and LDO is approximately 3 μA. This leakage is cancelled out by a minimal amount of light shining on the solar panel. This topic is further discussed in Chapter 10.

ZERO LEAKAGE STORAGE MODE

During storage, the energy harvesting system is not harvesting enough energy to sustain perpetual operation. If the system is allowed to run during storage, all energy will eventually be depleted, potentially over-discharging and causing damage to sensitive energy storage elements such as a thin-film battery. The solution is to create a safe "storage mode" that disconnects the energy storage element from the system until activated. In this design, the shunt battery charger with a battery disconnect feature provides protection against over-discharge during storage or when a brownout condition is detected. The battery is automatically disconnected from the system if the reserve voltage drops below 2.7 V.

USB QUICK CHARGE

The energy harvesting supply has the ability to quickly charge the energy storage medium when plugged into USB. A fully depleted system can be restored to full energy in under 30 minutes using this method. If USB power is not available, a fully depleted system will charge up in 2 to 24 hours based on the available light level.

Chapter 5: Data Acquisition

A primary function of the wireless sensor node is to collect information from its immediate environment and relay the information to a central receiver. This requires the node to have an analog data acquisition system. The energy harvesting wireless sensor in this design uses a 10-bit analog to digital converter for measuring temperature, illumination, and reserve voltage.

TEMPERATURE

Temperature is measured using the Si1012's on-chip temperature sensor. The transfer function of the temperature sensor is shown in Figure5.A. The temperature sensor output is internally routed to the ADC input through an analog multiplexer.

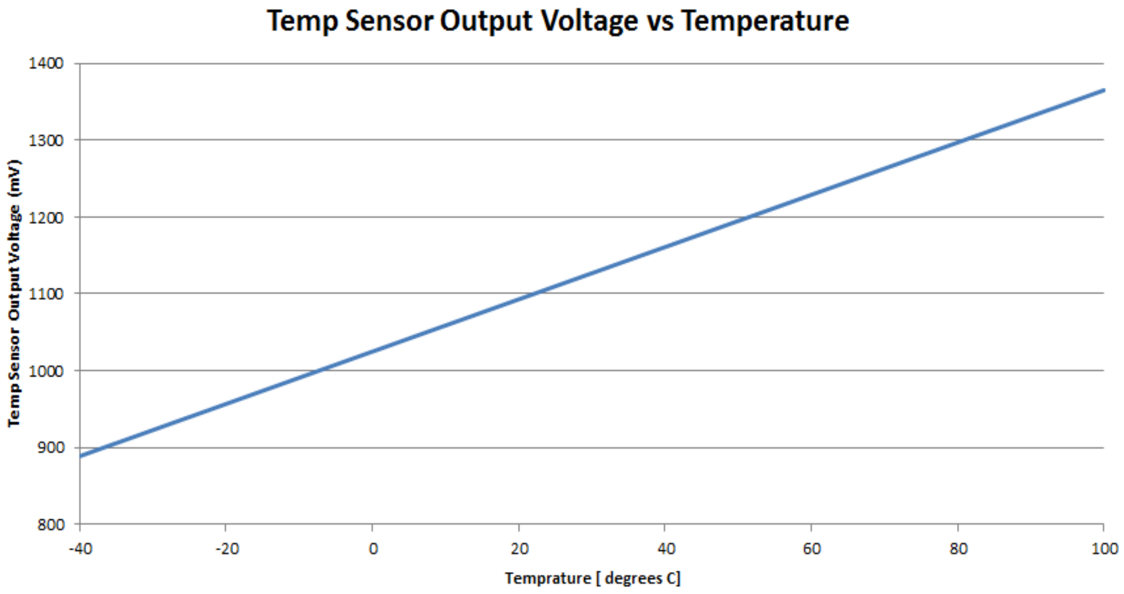

Figure 5.A: Temperature Sensor Output Voltage vs. Temperature

ILLUMINATION

The illumination level is determined by measuring the output current of the solar cell. One of the features of the Sanyo amorphous solar cells is that their output current is proportional to illumination. This allows them to be used as ambient light sensors in addition to their primary function as power sources. Figure 5.B shows the output current of the Sanyo AM-1815 solar cell vs. illumination.

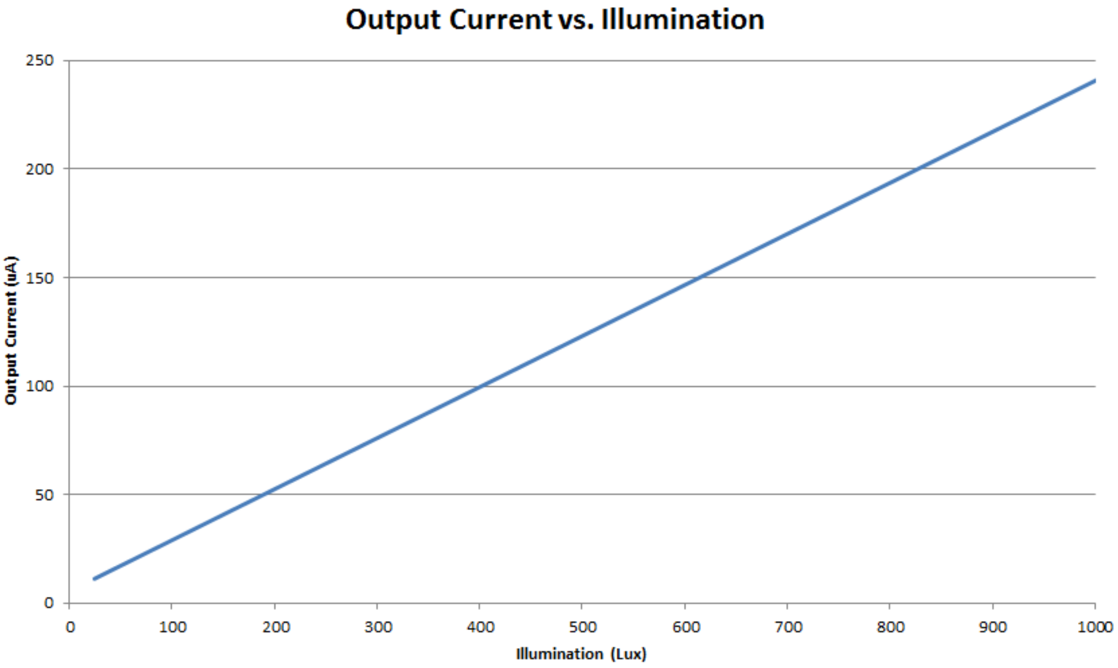

Figure 5.B: Solar Cell Output Current vs. Illumination

A solar cell's output current is linear at high illumination levels. Below 50 Lux, the output current exhibits non-linearity and may begin sinking current if a voltage potential is applied to its output. The parasitic current that flows in a solar cell independently and in the reverse direction of its photocurrent is called dark current. Dark current is typically negligible in most applications but can be a significant source of leakage in an energy harvesting system with limited reserve energy. In this design, dark current is blocked from depleting the system's energy reserves by using a low leakage schottky diode. Figure 5.C shows how the schottky diode is used to allow the solar cell to energize the system when light is available and block reverse current in darkness.

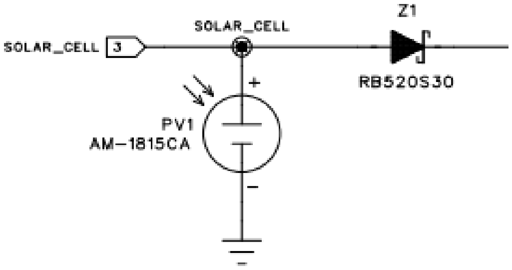

Figure 5.C: Using a schottky diode at solar cell output to block dark current

The solar cell's output current also has a load dependency and will be limited if the load impedance is too large or the energy harvester's reserve voltage approaches the solar cell's open circuit voltage. The energy harvesting system presents a very low impedance load to the solar cell when its energy reserves are depleted and a very high impedance load when fully charged. To accurately measure the solar cell's output current for the purpose of determining illumination, a mechanism for fixing the load impedance independently of the energy harvester's charge state is required.

To achieve a fixed load impedance, a resistor network with an equivalent shunt resistance of 10 kΩ is switched in at the beginning of the current measurement. This reduces the load impedance and pulls down the solar cell output voltage to allow accurate current measurement. The schottky diode shown in Figure 5.C comes in very handy during this current measurement because it blocks reverse current flow from the energy harvester and ensures that all current that flows through the resistor network is coming from the solar cell.

A secondary function of the resistor network, shown in Figure 5.D, is to convert the solar cell's output current to a voltage which can be easily measured using the ADC on the microcontroller. A resistor network was used instead of a single resistor to overcome the maximum analog voltage restrictions caused by the 2.7V I/O voltage and the threshold voltage of the n-channel pass transistor. With a 10 kΩ load resistance, the solar cell output voltage cannot exceed 3.3V even under the brightest light conditions. The analog voltage in the middle of the divider does not exceed 1.65V when the active high enable signal connected to the MOSFET gates is asserted. The resistor network is switched out of the circuit after the current measurement has been taken.

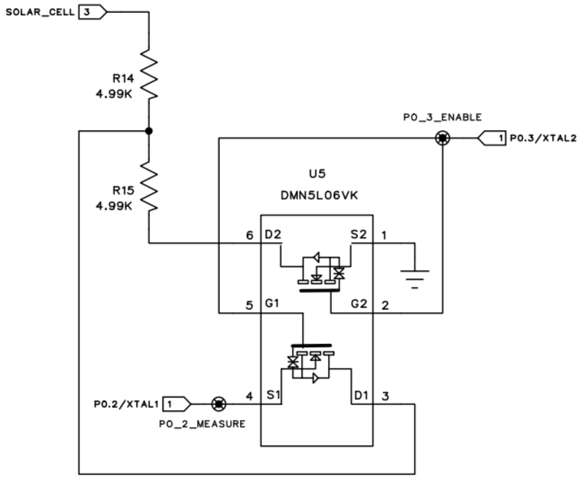

Figure 5.D: Solar cell current measurement circuit

RESERVE VOLTAGE

Measuring the reserve voltage in this design provides some challenges because the reserve voltage is higher than the supply voltage of the microcontroller and using a traditional resistor divider to generate a reduced sense voltage would discharge the storage medium. Nonetheless, having knowledge of the reserve voltage is very important in an energy harvesting system because it provides an early warning of power failure and the device can safely enter a low power mode until the system is replenished with energy. A method to measure the reserve voltage without discharging it would need to be developed for this energy harvesting design.

The circuit shown in Figure 5.E was designed to measure the reserve voltage. It uses a resistor network and 4 mosfets to measure the reserve voltage without significantly disturbing it. With this circuit, there is a tradeoff between discharge current during the measurement and measurement speed. The optimum value will minimize the discharge current during the measurement yet allow sufficient current to flow as not to prolong the measurement time as a result of an increased settling time. The impedance of the resistor network was set at 300 kΩ which allowed a reasonable settling time while maintaining a low discharge current.

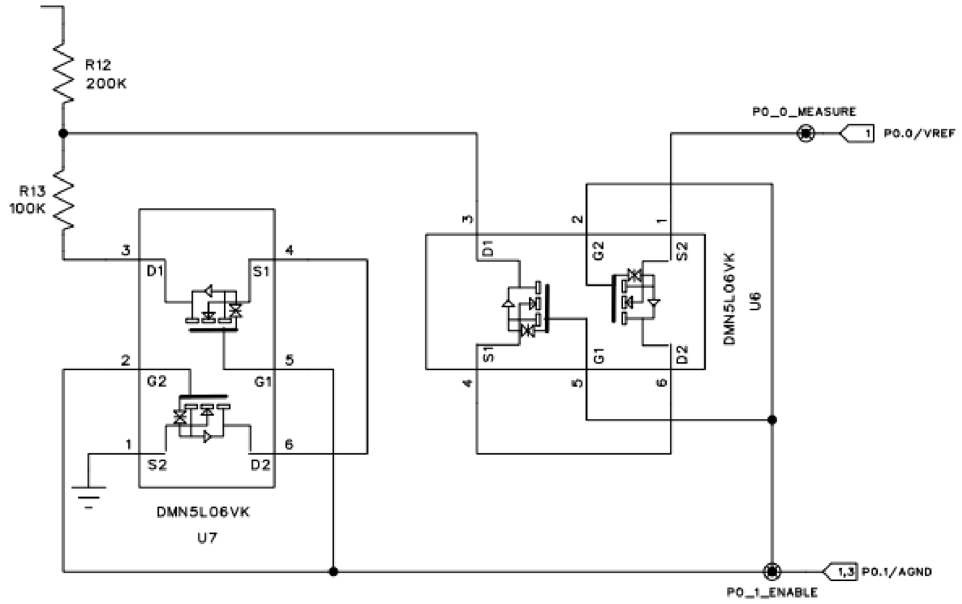

Figure 5.E: Reserve voltage measurement circuit

The key benefit of this reserve voltage measurement circuit is its ultra-low leakage current when turned off. A single DMN5L06VK transistor is specified to have a maximum leakage of 60nA at V_{GS} = 0V, which would be a significant amount of continuous leakage for the measurement circuit. To reduce this leakage, a second series transistor is placed in the circuit with the bottom transistor appearing as a large source resistance to the top transistor as shown in Figure 5.F.

If the gate of the top transistor was tied to its source, the effective impedance of the transistor pair would double and the maximum leakage would be reduced to 30 nA. To achieve even further reduction in leakage, the gate of the top transistor is tied to the source of the bottom transistor, allowing any leakage current flowing through the branch to generate a negative V_{GS} for the top transistor, virtually eliminating the flow of current. Since the impedance of an off transistor is very high, the slightest amount of leakage current is sufficient to produce a negative V_{GS} for the top transistor. This circuit has achieved a leakage of 3 nA as a result of using this transistor configuration, a factor of 20X less leakage than when using a single transistor to disconnect the resistor network.

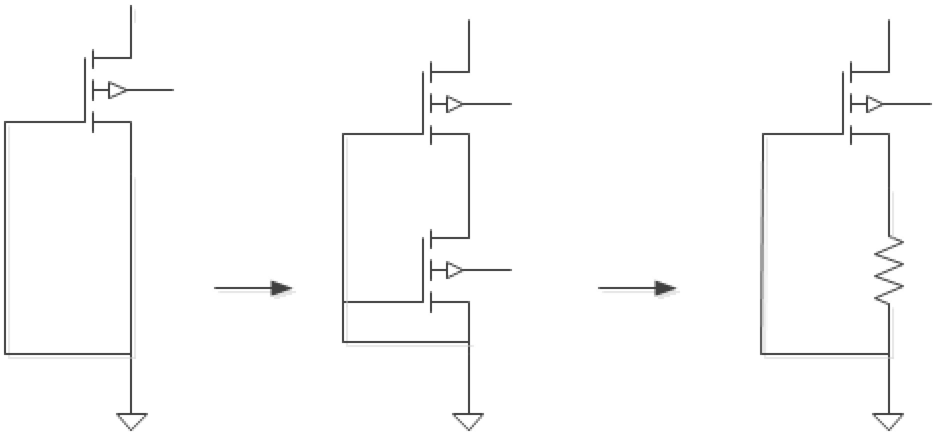

Figure 5.F: Using a second mosfet as a source resistor to reduce leakage

The same principle using the two additional diodes, U6, was used to minimize any leakage current into the microcontroller’s sense pin during the time when the microcontroller is unpowered and the sense pin can present a leakage path to ground. When the microcontroller is powered, its sense pin is configured as a high impedance analog input.

Chapter 6: User Interface

The user interface on the energy harvesting node is very simple and consists of a push-button switch, one green and one red LED indicators, and a power select switch. A PC based graphic user interface (GUI) is used to display the data collected by each node.

RESERVE VOLTAGE INDICATOR

The energy harvesting node flashes the LEDs three times to indicate the approximate energy remaining in reserve. The approximation is calculated based on the reserve voltage and the level is indicated using the LED color. Three green pulses indicate that there is more than 75% of energy capacity in reserve. Two green pulses followed by one red pulse indicate more than 50% of energy capacity is in reserve. One green pulse followed by two red pulses indicates that more than 25% of energy capacity is in reserve. Three red pulses indicate that reserve energy has dipped below 25%. The energy harvesting note will immediately go into a low power mode after performing the indicator function if it detects that the reserve energy had dropped below 25%.

TRANSMISSION GOOD INDICATOR

The green LED is used as a transmission good indicator when there is greater than 75% of energy capacity in reserve. The indicator is turned on for a period of 10 milliseconds after the receipt of the acknowledge indicating the successful transmission of a data packet. When the reserve energy drops below 75%, the transmission good indicator function is automatically disabled.

TRANSMISSION FAILED INDICATOR

The red LED is used as a transmission failed indicator. The indicator is turned on for a period of 10 milliseconds when the acknowledge packet indicating a successful transmission is not received after the specified timeout. Unlike the transmission good indicator, the transmission failed indicator is enabled even if there is less than 75% of energy capacity in reserve.

PUSH BUTTON SWITCH FOR USER INPUT

The push button switch is used to wake the energy harvesting node up from its lowest power sleep mode and begin transmission. Once awoken, the energy harvesting node will transmit for a period of 1 minute per button press. Pressing the button 5 times will result in a transmission time of 5 minutes.

POWER SELECT SWITCH

The power select switch has three settings: SOLAR, AUX, and USB. The SOLAR setting enables the charging circuitry and power the microcontroller from the reserve energy in the system. The USB setting powers the microcontroller from USB, and allows the internal reserve energy to quick-charge over USB, and enables the debug interface to the microcontroller. The AUX setting disables the charge circuitry and allows the system to be powered from an auxiliary supply. When the charge circuitry is disabled, the energy storage medium is disconnected from the system allowing it to preserve its charge in a zero-current ship mode. See the appendix for a detailed system schematic showing how the 4-pole power select switch re-configures the system.

PC BASED GUI FOR DATA DISPLAY

The PC-based graphic user interface developed for this project is shown in Figure 5.G. For up to four nodes, the GUI displays the current temperature, illumination, and the percent of system's energy storage capacity in reserve. The GUI also displays the value of RSSI reported by the RF receiver for each node. This can help the user determine the approximate distance between the transmitter and receiver. This graphic user interface was designed by the author's colleague in collaboration with the author with respect to the underlying protocol for data transfer.

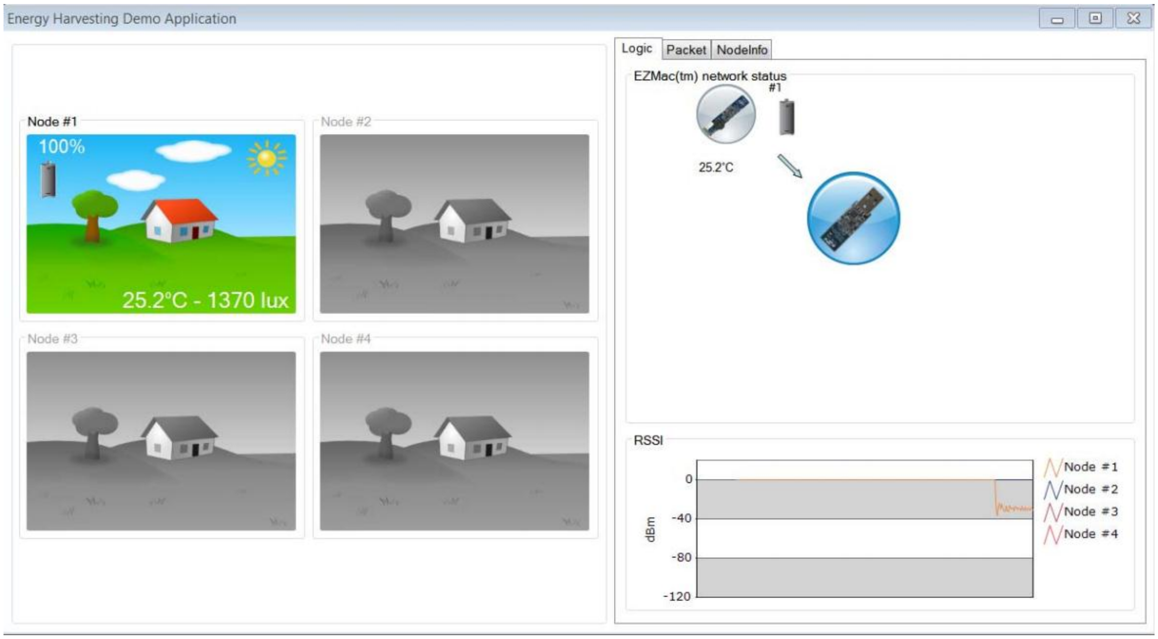

Figure 5.G: Energy Harvesting Graphic User Interface

Chapter 7: Software

Software is a major component of the energy harvesting node. It is responsible for managing the user interface, collecting data, and transmitting it over the RF interface. The starting point for software development in this project was the RF-to-USB reference design, which uses the EZMacPRO™ RF communication stack provided by Silicon Laboratories for basic communication. Changes were made to both the application layer and the low level functions to make it compatible with the energy harvesting node.

The software running on the energy harvesting node plays a major role in the power efficiency of the system. Software designed to minimize power consumption will enhance reliability and robustness of the energy harvesting system. The software in this design was optimized to take advantage of the low power features of the underlying hardware and minimize total system power.

CREATING A FUNCTIONING PROTOTYPE

One of the main functions of the energy harvesting prototype board shown in Figure 2.C is to expedite software development while the energy harvesting node hardware was being designed and fabricated. The prototype hardware is based on the RF-to-USB reference design board, which is normally powered from a single AAA battery.

The RF-to-USB reference design software required a power source with a large capacity and the ability to source high peak currents, such as an alkaline battery, and used the Si1014's DC-DC converter to boost the supply voltage up to 3.3V. The need to utilize the DC-DC converter prevented the microcontroller from utilizing its RTC sleep mode and instead entered into a higher power suspend mode any time the EZRadioPRO peripheral needed to be powered. Finally, the large available capacity allowed the software to be optimized for code size and maximum RF range, not low power.

The RF-to-USB software required several modifications to run from an energy harvesting supply, primarily focused on reducing power consumption. The first major change was disabling the DC-DC converter and allowing the system to use RTC sleep mode instead of suspend. Next, all software polling was replaced with event-based transitions between RTC sleep and active mode. Finally, the application layer was modified to meet the data collection and transfer requirements of this design and more power saving optimizations were performed.

EVENT DRIVEN SOFTWARE ARCHITECTURE

The software architecture used for this design is event driven. This allows the microcontroller to remain in a low power state except for the brief time when executing an event handler. The event driven architecture significantly reduces the average supply current of the microcontroller. Figure 7.A shows how the software transitions the embedded system between its three primary power states based on system events.

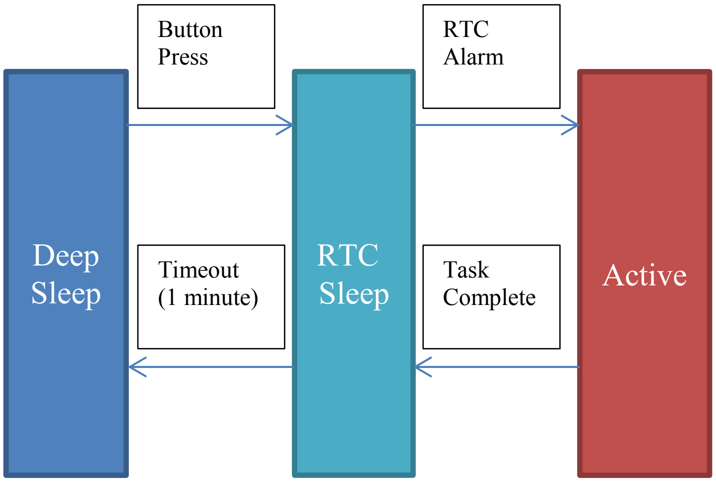

Figure 7.A: Event based system state transition

The embedded system spends most of its time in its deep sleep mode and transitions to the RTC sleep mode when the push button is pressed. The microcontroller wakes up once a second to handle the RTC alarm by switching to active mode and transmitting a data packet. As soon as the transmission is complete, the microcontroller switches back to the RTC sleep mode. After a 1 minute timeout, the microcontroller transitions into deep sleep awaiting the next button press. The time between push button presses can be hours to days for this embedded system.

LOW POWER MODES

The embedded system has three power modes: deep sleep, RTC sleep, and active. Deep sleep mode is the microcontroller's lowest power mode and it is where the microcontroller's RF peripheral is completely powered down, all clocks including the RTC are disabled, and an external stimulus is required to wake up. The microcontroller's supply current in this mode is 60 nA and the external stimulus used to wake up is the push button switch. It takes approximately 20 ms to wake up from deep sleep mode.

The RTC sleep mode is used as an intermediate low power mode for the microcontroller, allowing its supply current to be reduced to approximately 1.2 μA. From RTC sleep, the microcontroller can return to the active mode within 2 μs, making this mode ideal for implementing short delays required when initializing the radio. In fact, during wakeup from deep sleep, the MCU enters active mode, initiates a radio wakeup, and then enters RTC sleep to wait until the radio initialization is complete.

In this system, active mode is defined as either the microcontroller executing code, the RF transmitter is active, or the RF receiver is active. The microcontroller requires 3.5 mA when executing code, the RF transmitter requires 29 mA, and the RF receiver requires 19 mA. Due to the limited peak current available to the system, only one of the three primary current consumers are enabled at a time.

RESERVE VOLTAGE RECOVERY

The reserve energy storage medium is very good at supplying the system with its average supply current, however, it cannot provide the instantaneous charge requirements of the system in active mode due to its high output impedance. A 100 µF capacitor has been added to the output of the battery in order to provide the instantaneous energy required by the system's active mode.

The large decoupling capacitor allows the system to stay in active mode for a finite amount of time before running out of energy. The amount of time the system can remain in active mode depends on the starting reserve voltage and supply current in active mode. Upon entry into active mode, the load current instantaneously steps up to support the system demand and the reserve voltage begins to drop.

Figure 7.B shows a model of the reserve voltage while the system is transitioning to active mode from a low power state. The load current is modeled as a step function at the start of the simulation and the energy storage medium is modeled as an ideal voltage source and equivalent output impedance.

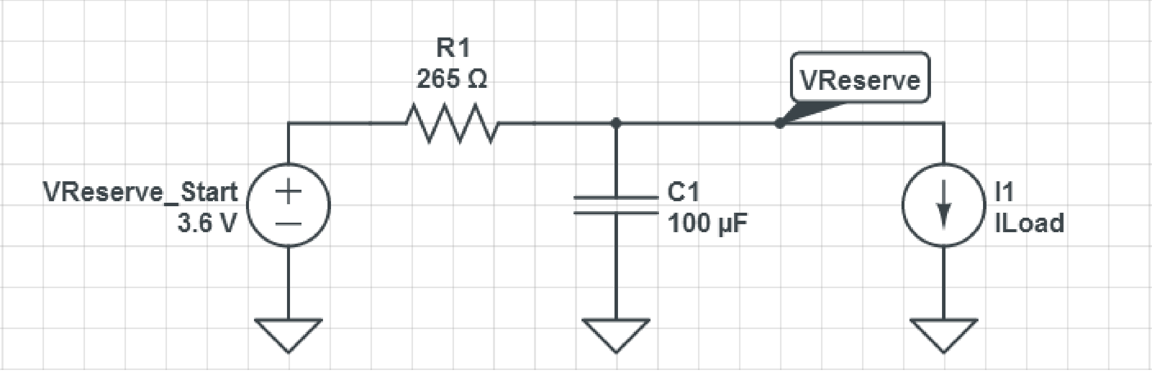

Figure 7.B: Model of Reserve Voltage While Transitioning to Active Mode

During normal operation, the starting reserve voltage is equal to the voltage of the storage medium, which can be between 4.1 V to 3.6 V depending on the amount of energy held in reserve. The starting reserve voltage and source impedance been conservatively modeled to be with the energy reserves almost depleted to ensure that the resulting calculations are valid across the entire operating range and to provide additional margin when operating with a higher levels of reserve energy.

The supply voltage monitor connected to the reserve voltage will power down the system if the reserve voltage drops below 3.0 V. To prevent an unintended power down, software must ensure that tasks performed in active mode are of sufficiently short duration so as not to cause the reserve voltage to dip below 3.0 V.

Figure 7.C shows the reserve voltage decay over time when the system is in active mode. The maximum amount of time that the microcontroller can spend in active mode is approximately 48 ms if it is only executing code, 3 ms if the receiver is enabled, and only 2 ms if the transmitter is enabled at maximum transmit power.

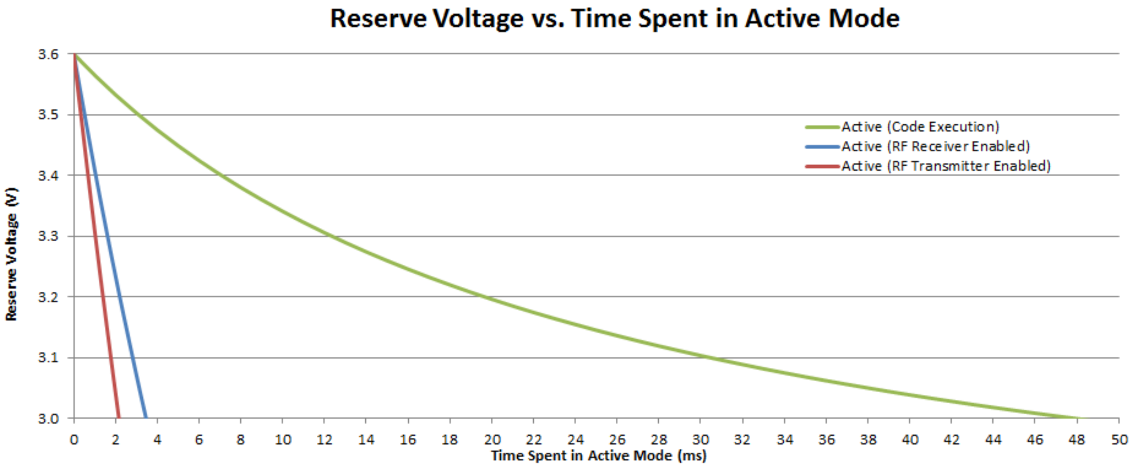

Figure 7.C: Reserve Voltage vs. Time Spent in Active Mode

When necessary to perform CPU-intensive tasks that require the microcontroller to spend large amounts of time in active mode, software will break up the task into smaller tasks and pause for approximately 10 to 20 milliseconds in-between each small task to allow the storage medium to replenish the charge in the capacitor. This method of reserve voltage recovery is used while initializing the RF transceiver over the SPI interface after waking up from deep sleep and after RF data transfer.

RF DATA RATE, ACKNOWLEDGMENT, AND LISTEN BEFORE TALK

The RF transmitter and receiver can only remain enabled for a short duration before placing the system at risk of being powered down by the supply monitor. For this reason and for the fact that a faster transmission will reduce the average current required by the system, the fastest available data rate of 128 kbps was selected. This allowed the data collected by the sensors to be transmitted in less than 1 ms.

The EZMACPRO™ software stack supports both acknowledgments and listen before talk to maximize data integrity and minimize packet loss. The acknowledgment required the receiver to be enabled for approximately 1 ms after a transmission is complete and listen before talk required the receiver to be enabled for approximately 5 ms before the transmission started. The energy harvesting node software implements acknowledgements and disables the listen before talk feature due to its high power requirements. Since the interval in between packet transmissions on the energy harvesting system is very low, the probability of data loss as a result of a collision is very low. Since acknowledgments are enabled, the transmitter that detects data loss in the rare event of a collision may opt to re-transmit the data.

DYNAMICALLY ADJUSTED TRANSMIT POWER

Since the receiver must be enabled immediately after transmission is complete in order to receive the acknowledgment, reserve voltage recovery cannot be performed in-between the transmission phase and the reception phase of the data transfer. To minimize the risk of being powered down by the supply monitor, maximum transmit power is only enabled only when the reserve medium has at least 75% of its capacity in reserve. At all other times, the transmitter power is reduced to save energy. The range of the RF transceiver still exceeds the minimum specified range for this design when operating at the reduced transmit power.

Chapter 8: Hardware

The starting point for the hardware design in this project was the RF-to-USB reference design and the PCB design was progressing in parallel with the initial software development on the prototype. The hardware design process consists of schematic capture, component placement, layout, and prototype build.

SCHEMATIC CAPTURE

The schematic capture process started with the creation of a detailed list of modifications from the RF-to-USB reference design board. These changes were primarily in the power supply and data acquisition circuits described in Chapter 4 and Chapter 5. The user interface remained the same primarily for software compatibility between the two platforms. The final schematics for this design are available in the appendix.

LAYOUT

The starting point for the layout was the RF-to-USB reference design board shown in Figure 8.A. This design includes an RF layout with printed antenna and a user interface consisting of a push-button switch and two LEDs. A significant amount of circuitry for the energy harvesting power supply and data acquisition circuits would need to be added to the board. The RF portion of the design is very sensitive to layout and one of the primary challenges in this PCB design is how to add the additional circuitry to the system without affecting the RF performance.

The next step in the layout was creating a component placement. Judging from the number of components that need to be added to the design, including a large solar cell that needed top layer surface area, the board size would have to be expanded. To minimize disturbance to the RF circuit, the PCB would grow to the sides and to the bottom leaving the RF layout and PCB antenna intact.

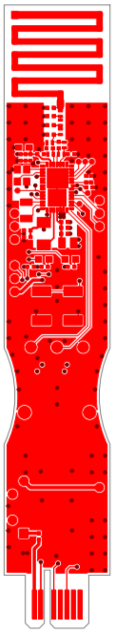

Figure 8.A: Starting Point for Layout, RF-to-USB Reference Design

The PCB antenna requires a keep out area on both sides of the board spanning the entire width of the board. This allows the antenna to be omnidirectional as any copper placed directly in the antenna's transmit path will create spots where the signal will be weak as it must travel around the copper feature. Figure 8.B shows the keep out area on the energy harvesting node board designed to achieve uniform signal coverage in all directions around the antenna. This figure also shows how the PCB was widened and lengthened to accommodate the additional energy harvesting circuitry.

The energy harvesting supply circuitry was primarily located on the bottom side of the PCB. This allowed the energy harvesting supply circuitry to be easily debugged by simply turning the board over. Silkscreen was added to both sides of the board to simplify component identification.

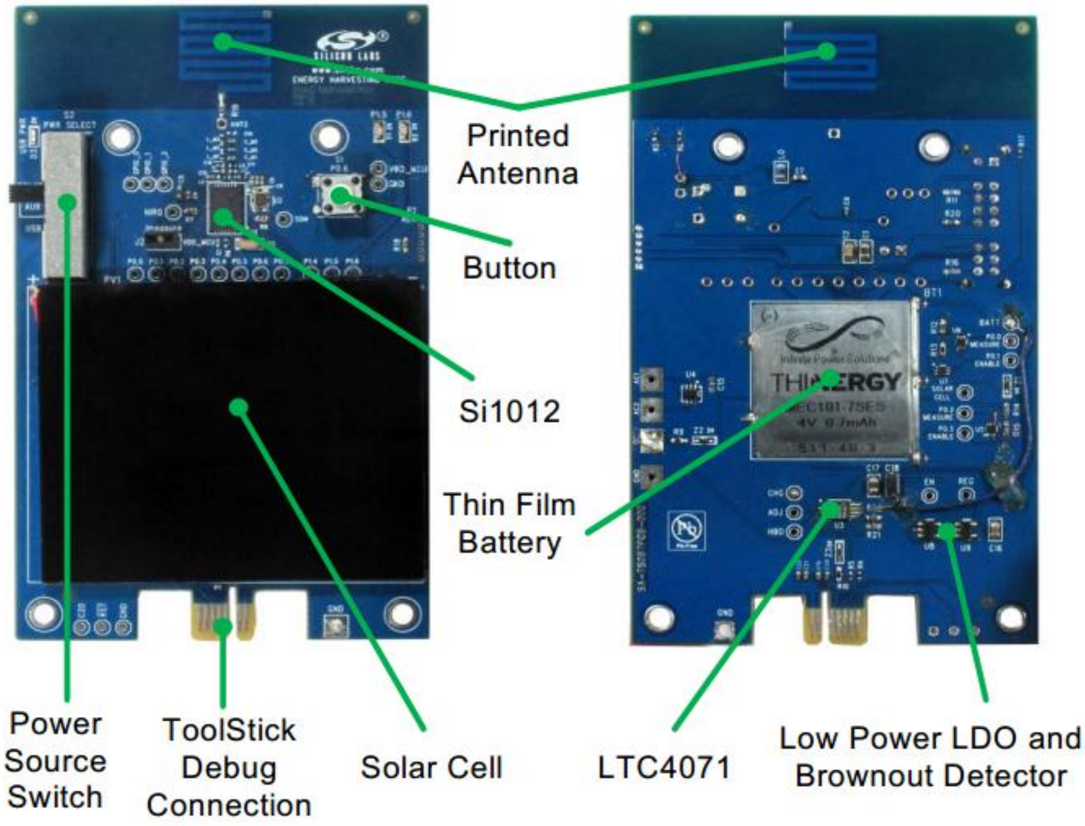

Figure 8.B: Energy Harvesting Board Layout

PROTOTYPE BUILD

After the component placement was complete, the design was submitted to the author’s colleague for final routing, flood, and Gerber file generation. A prototype build was subsequently manufactured and assembled.

RESULTS AND CONCLUSION

Chapter 9: Evaluating Initial Prototype

At the time the boards from the initial prototype build arrived, the software design was well under way and was used to validate the hardware. The hardware validation consists of functional verification, performance optimization, user interface testing, and finally releasing the hardware design to production.

FUNCTIONAL VERIFICATION

The functional verification begins with a continuity check before power is ever applied to the board. The continuity check verifies that there is an electrical connection between the nodes that should be connected in the design. Any manufacturing errors resulting in open connections or connections shorted to power or ground can be repaired by removing unwanted traces and making blue wire connections.

Careful layout and a good review process can help reduce errors, but some errors will still propagate through the pre-manufacturing verification. It is essential to review the design carefully for errors at each stage to catch any design or layout errors. The earlier an error is found, the less costly it will be to fix it. In this design, a layout error resulting in an incorrect footprint being used for the push-button switch was identified in functional verification of the initial prototypes. Luckily, it is easy to bend the leads on a push-button switch and get it to fit in an incorrect footprint so this did not delay the rest of the verification effort and would be fixed in the next iteration of the board.

The next step was to power up the board and verify the functionality of each block. The microcontroller had no problems establishing a debug connection to development environment, blinking the LEDs, and transmitting and receiving RF packets. The data acquisition circuits appeared to be functional because they were resulting in ADC codes within the expected range when their output voltages were digitized. The energy harvesting supply also appeared to properly charge the storage medium and the RF transmitter and receiver were subjected to a standard test that measures transmit power and receive sensitivity. The results were on par with the RF-to-USB board so things were looking good from a functionality perspective.

A power measurement test indicated that there was a leakage path somewhere in the design. The leakage path was traced to the data acquisition circuits and after debugging, it appeared that the mosfets used to disconnect the resistor networks were used as symmetrical devices without regard to the direction of the body diode. In an ideal mosfet, the source and drain are identical, however, a real mosfet cannot be manufactured without the parasitic body diode.

The body diode only allows the mosfet to block current in one direction when turned off. To block current in both directions, two mosfets may be placed back to back with their body diodes in opposing directions. In this design, current only needs to be blocked in one direction in the off state so no additional circuitry was required however the source and drain needed to be swapped on some of the mosfets used. This change was verified with blue wires on the boards from the initial prototype build.

PERFORMANCE OPTIMIZATION

Now that the design had been validated and deemed functional, it was time to optimize its performance. The first optimization involved determining the optimum capacitor value to use for decoupling the reserve voltage. It was determined that using the next smaller size capacitor, 50 μF, would generate a high risk of shutting down the system during RF transmission and using a larger capacitor would be cost prohibitive. The optimum value for the decoupling capacitor was 100 μF.

The next parameter to be optimized was the transmit power. It was observed that the transmit power setting on the transmitter had a direct impact on range. It was determined that it is best to transmit at maximum power if the system had enough energy to support such a transfer and dial down the transmit power only when the reserve voltage was running low.

The regulator voltage was the next parameter set for optimization. The MCU can operate from 1.8 V to 3.6 V, so there was a wide range of potential voltages. In general, the lower the LDO voltage, the lower the system power consumption will be. Through range testing, it was determined that voltage did not significantly impact the RF range so a low regulator voltage is ideal. The optimum regulator voltage was determined to be 2.7V because it reduced the power dissipated in the RF circuit and was high enough so as not to affect the analog performance of the data acquisition circuits.

The reserve voltage monitor used to power down the system when the reserve voltage drops below 3.0 V has a programmable delay element before powering on the system. This delay element was set to be approximately 100 ms to minimize the potential for oscillation and at the same time not unnecessarily prolong startup time. The threshold voltage of the monitor is set at 3.0V to ensure a sufficient margin above the LDO output voltage. The LDO used in this design enters a high current state when its input begins to drop out, therefore the extra margin is required to ensure the regulator never enters into its drop out region of operation.

The final optimization was calibrating the illumination measurement with an MS6610 lux meter. This allowed the measurements reported by the node board to match the measurements obtained from the handheld lux meter. The temperature measurement used calibration data obtained during microcontroller production. The reserve voltage measurement does not require calibration because it is voltage based.

USER INTERFACE TESTING

After the system operation had been optimized, it was time to check the user interface. The first parameter that could be adjusted is the amount of time the system would transmit after being woken up. After several usability experiments, it was determined that the system needed to transmit for 1 minute each time it is awoken. The user interface software was designed such that it would transmit for 1 minute per button press, with packets being sent once a second.

The next parameter dealing with the user interface is the LED on time when blinking. The LEDs are used as indicators and it is important that they be clearly visible. It is also important that they do not remain enable for a long time so as to minimize power dissipation. It was determined that keeping the LEDs on for 10 ms would create a sufficiently visible blink without dissipating too much energy.

The initial power on requires at least 200 lx shining on the solar cell to charge up the reserve voltage bypass capacitor. The board was tested in various indoor and outdoor lighting conditions to ensure that the system was able to reliably start up in less than ideal lighting conditions.

TESTING FOR INTERFERENCE AND INTEROPERABILITY

One of the design goals of this project is interoperability and multi-node capability. Five prototype boards were tested in a room with four other RF-to-USB reference design boards operating at the same frequency. No interference was detected and the systems operated as designed. Various nodes were also tested with multiple receivers and all operated as designed.

RELEASE TO PRODUCTION

One board revision was required to fix the errors found in the initial prototype and then the hardware was released to production.

Chapter 10: Power Analysis

One of the most important characteristics of an energy harvesting system is its power consumption. In this chapter, we will examine the power consumption of the final energy harvesting hardware and software that has been released to production.

POWER PROFILE

The energy harvesting node spends most of its life in deep sleep mode, where the entire system is drawing approximately 3 µA. Once it exits sleep mode, the microcontroller dynamically switches between RTC Sleep and Active Mode. In Active Mode, the total system supply current is 29 mA when transmitting, 19 mA when receiving, and 4.2 µA in RTC Sleep. In this analysis, the average current contribution from the microcontroller's code execution is considered negligible and accounted for by rounding the transmitter and receiver on time up to the nearest millisecond.

Figure 10.A shows the power profile of the energy harvesting system while transferring data. Data is transferred once per second at an average current of 52 µA. The system's 700 µA-H energy storage medium has sufficient capacity to allow the system to continuously transmit data for 13 hours or remain in deep sleep mode for over 9 days after all power sources have been removed.

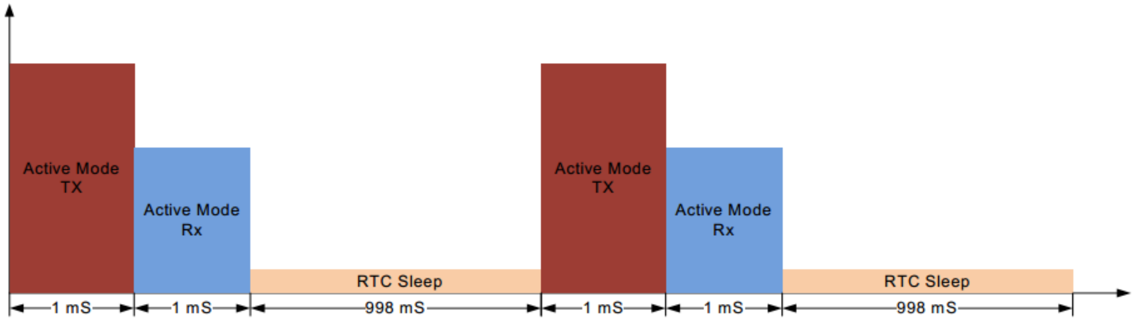

Figure 10.A: Power Profile During Data Transfer

PERPETUAL OPERATION

A well designed energy harvesting system will balance its harvested energy with the energy requirements of the system to achieve perpetual operation. The internal reserve voltage is primarily used as a buffer to help meet the system's instantaneous energy needs and to power the system during periods when harvested energy is not available.

In deep sleep mode, the system requires 3 μA from the solar cell to equalize the losses resulting from the charging circuit. The solar cell can provide this current with less than 50 lx of light shining on its surface. This means that if there is sufficient light for a person to walk around and do basic tasks in a dark room, this amount of light is enough to keep the energy harvesting system in perpetual operation in deep sleep mode.

When transferring data continuously, the system requires 52 μA of average current from the solar cell to maintain perpetual operation. The solar cell can provide this current with less than 200 lx of light shining on its surface. Dim indoor lighting can produce enough light to keep the energy harvesting node in perpetual operation while transferring data continuously.

Under typical operation, the system will not be transferring data continuously nor will it remain in deep sleep indefinitely, but will most likely experience a combination of both modes. It is also very likely that the system will be exposed to high amounts of light during parts of the day and low amounts of light during other parts, such as night time. As long as the input power is greater than or equal to the output power, the energy harvesting system will remain in perpetual operation.

Chapter 11: Conclusion

SUMMARY OF PROJECT AND RESULT

This report details the design and development of an energy harvesting wireless sensor from concept to production. Each phase of the design process was described and an energy harvesting wireless sensor node, shown in Figure 11.A, was manufactured, tested, and released to production. The energy harvesting node resulting from this work has an average current of 52 μA and is capable of perpetual operation when a dim indoor light source as low as 200 lx is available.

Figure 11.A: Energy Harvesting Node

FUTURE WORK

Future work in energy harvesting would include the addition of various harvesting sources such as mechanical, thermoelectric, or RF. Research into energy harvesting without a large energy storage medium, such as a light switch RF transmitter, would also complement this work and be the basis for future research in this area.

Appendix – Schematic

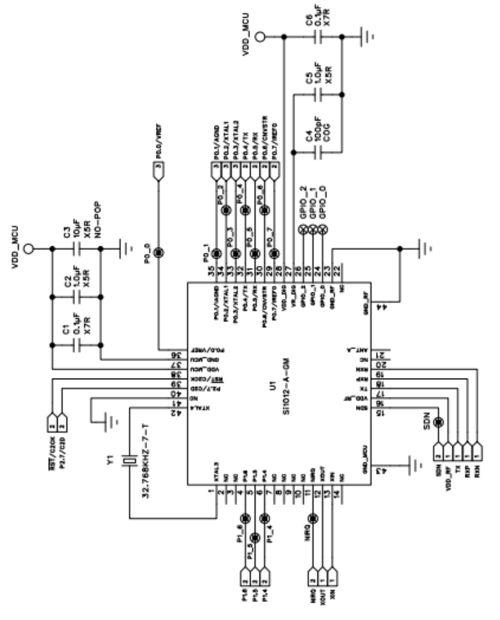

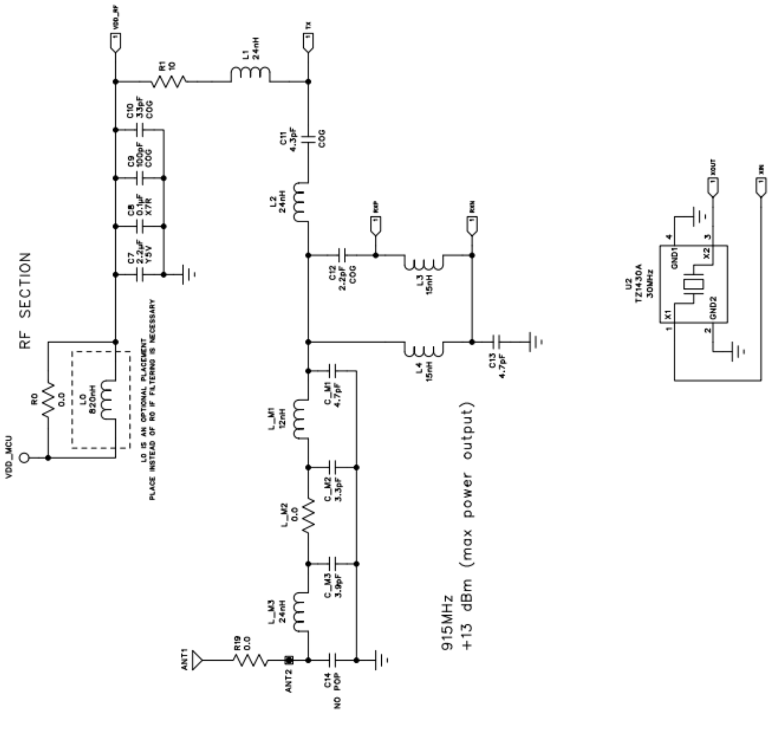

User Interface

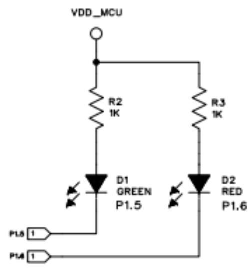

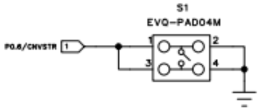

PORT I/O USAGE

P0.0 – Battery Voltage Measure (Analog Input)
P0.1 – Battery Voltage Measure Enable (Digital Output)
P0.2 – Solar Cell Voltage Measure (Analog Input)
P0.3 – Solar Cell Voltage Measure Enable (Digital Output)
P0.4 – UART TX (Digital Output)
P0.5 – UART RX (Digital Input)
P0.6 – Wake Up Switch (Digital Input)
P0.7 – EZRadioPRO Interrupt (Digital Input)
P1.4 – EZRadioPRO Shutdown (Digital Output)
P1.5 – Green LED (Digital Output)
P1.6 – Red LED (Digital Output)
P2.7 – C2D

Toolstick Programming / UART

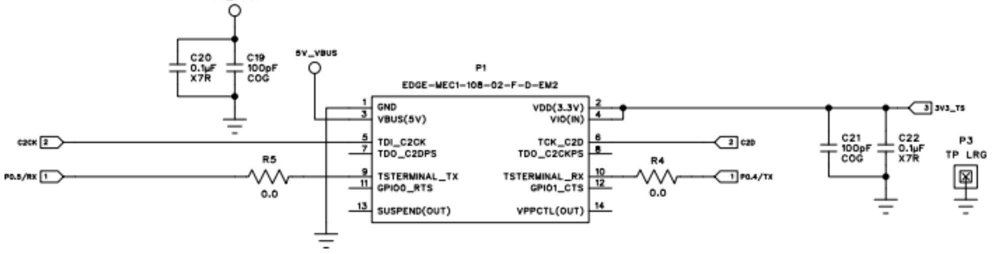

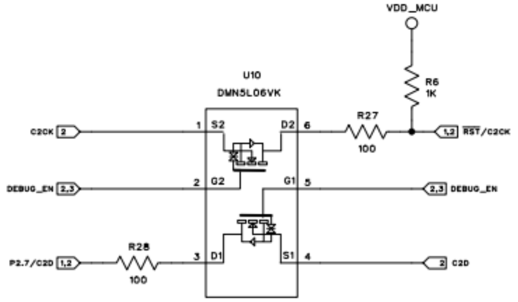

TESTPOINTS

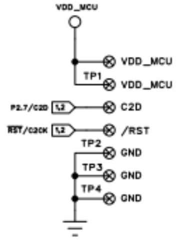

I/O Connections

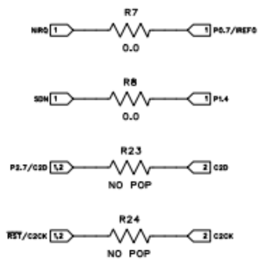

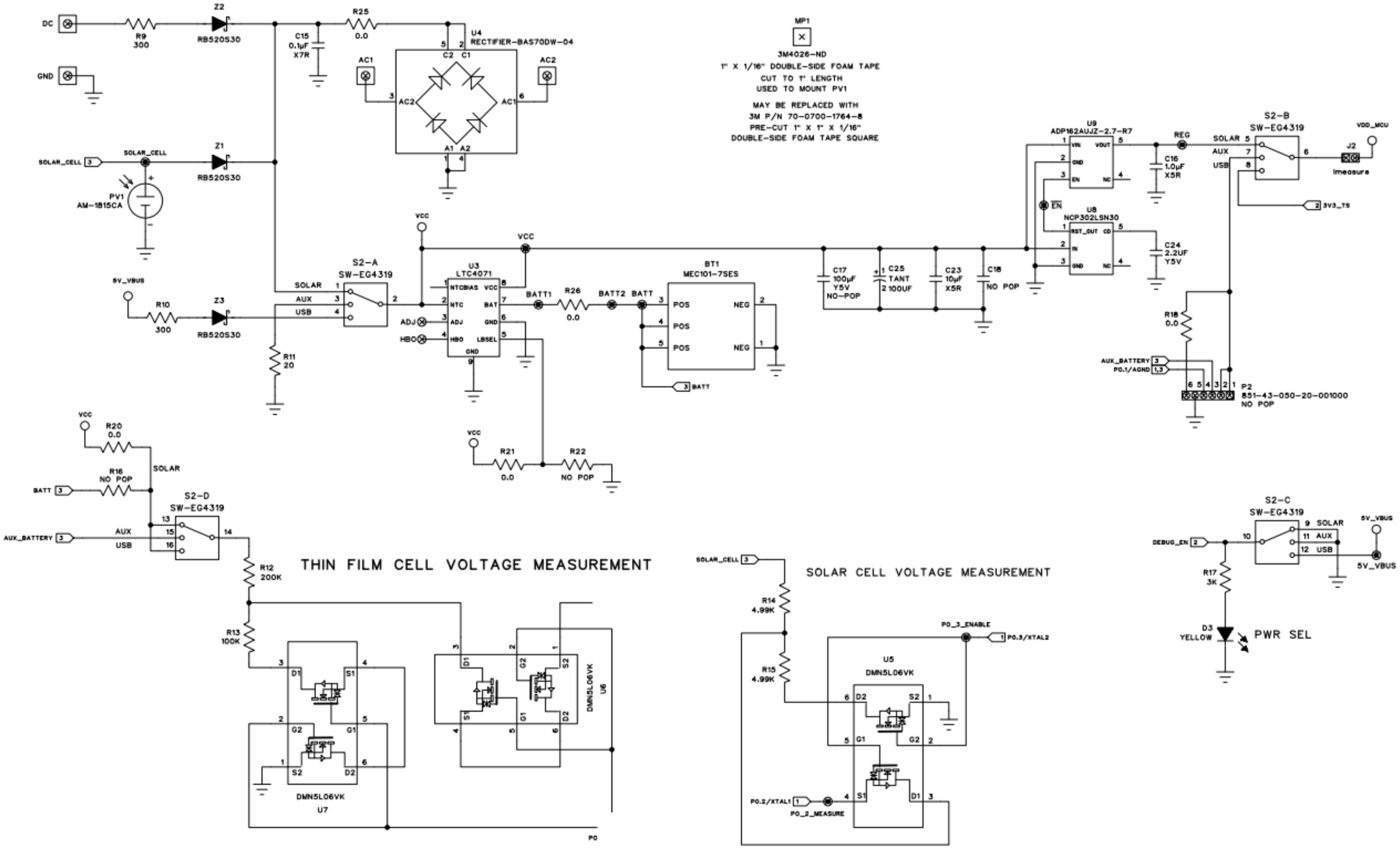
DC
GND
R9 300
Z2 RB520S30
C15 0.1μF X7R
R25 0.0
U4 RECTIFIER-BAS70DW-04
AC1
AC2
SOLAR_CELL
PV1 AM-1815CA
Z1 RB520S30
5V_VBUS
R10 300
Z3 RB520S30
R11 20
S2-A SW-EG4319
SOLAR
AUX
USB
VCC
U3 LTC4071
NTCBIAS
NTC
ADJ
HBO
GND
BAT
LBSEL
BATT1
R26 0.0
BATT2
BATT
BT1 MEC101-7SES
POS
NEG
R21 0.0
R22 NO POP
C17 100μF Y5V NO-POP
C25 TANT 100UF
C23 10μF X5R
C18 NO POP
MP1
3M4026-ND
1" X 1/16" DOUBLE-SIDE FOAM TAPE
CUT TO 1" LENGTH
USED TO MOUNT PV1
MAY BE REPLACED WITH
3M P/N 70-0700-1764-8
PRE-CUT 1" X 1" X 1/16"
DOUBLE-SIDE FOAM TAPE SQUARE
U9 ADP162AUJZ-2.7-R7
VIN
VOUT
EN
NC
U8 NCP302LSN30
RST_OUT
CD
IN
C16 1.0μF X5R
C24 2.2UF Y5V
REG
S2-B SW-EG4319
J2 Imeasure
VDD_MCU
3V3_TS
R18 0.0
AUX_BATTERY
P0.1/AGND
P2 851-43-050-20-001000 NO POP
R20 0.0
R16 NO POP
S2-D SW-EG4319
R12 200K
R13 100K
THIN FILM CELL VOLTAGE MEASUREMENT
DMN5L06VK
U7
U6
P0
SOLAR CELL VOLTAGE MEASUREMENT
R14 4.99K
R15 4.99K
U5 DMN5L06VK
P0_3_ENABLE
P0.3/XTAL2
P0.2/XTAL1
P0_2_MEASURE
S2-C SW-EG4319
DEBUG_EN
5V_VBUS
R17 3K
D3 YELLOW
PWR SEL

References

[1] Brunelli, D., et. al. "Design of a Solar-Harvesting Circuit for Batteryless Embedded Systems". IEEE Transactions on Circuits and Systems I., Vol.56, Issue 11. pp. 2519-2528, 2009.

[2] Chalasani, S. and Conrad, J.M. "A Survey of Energy Harvesting Sources for Embedded Systems". Southeastcon. IEEE, pp. 442-447, 2008.

[3] Lopez, J., et. al. "Fast-Charge in Lithium-Ion Batteries for Portable Applications". 26th Annual International Telecommunications Energy Conference, pp.19-24, 2004.

[4] Raghunathan, V., et. al. "Design considerations for solar energy harvesting wireless embedded systems". Fourth International Symposium on Information Processing in Sensor Networks, pp. 457-462, 2005.

[5] Roundy, S.J. "Energy Scavenging for Wireless Sensor Nodes with a Focus on Vibration to Electricity Conversion". PhD Dissertation, Electrical-Mechanical Engineering, University of California-Berkeley, 2003.

[6] Sanyo Amorphous Silicon Solar Cells/Amorphous Photosensors. [online]. Available: http://us.sanyo.com/Dynamic/customPages/docs/solarPower_Amorphous_PV_Product_Brochure%20_EP120B.pdf.

[7] Simpson, C. "Characteristics of Rechargeable Batteries". Texas Instruments. Available: http://www.ti.com/lit/an/snva533/snva533.pdf.

[8] Carmo, J.P, et. al. "Integrated thin-film rechargeable battery in a thermoelectric scavenging microsystem". International Conference on Power Engineering, pp. 359-362, 2009.

[9] Silicon Laboratories. "Si1010/1/2/3/4/5 Datasheet". [online]. Available: http://www.silabs.com/Support%20Documents/TechnicalDocs/Si1010.pdf.

[10] Silicon Laboratories. "RF to USB Reference Design 2 User's Guide". [online]. Available: http://www.silabs.com/Support%20Documents/TechnicalDocs/RF-to-USB-RD.pdf.

[11] Silicon Laboratories. "AN415 EZRadioPRO Programming Guide". [online]. Available: http://www.silabs.com/Support%20Documents/TechnicalDocs/AN415.pdf.

[12] Infinite Power Solutions. "THINERGY™ MEC101 Datasheet". [online]. Available: http://www.infinitepowersolutions.com/images/stories/downloads/controlled_documents/ds1001.pdf.

[13] Linear Technology. "Li-Ion/Polymer Shunt Battery Charger System with Low Battery Disconnect Datasheet". [online]. Available: http://cds.linear.com/docs/en/datasheet/4071fc.pdf.

Vita

Farris Bar was born in Cairo, Egypt and moved to Texas at the age of three. In 1998, he graduated from Cuero High School and then moved on to earn his B.S. in Electrical Engineering from the University of Texas at Austin in 2002. Farris is currently a Senior Applications Engineer at Silicon Laboratories and specializes in ultra-low-power system design, embedded ethernet, and designing systems around the 32-bit ARM Cortex microcontroller. His hobbies include exercising, photography, pets, water sports, and enjoying nature in various parts of the world.

Permanent Electronic Address: farris.bar _at_ alumni.utexas.net
This report was typed by the author.